

Non-contact vibration measurement based on an extrinsic Fabry–Perot interferometer implemented using arrays of single-mode fibres

Tarun Kumar Gangopadhyay¹

University of Sydney, School of Electrical and Information Engineering, Sydney, NSW 2006, Australia

E-mail: tkgee@hotmail.com

Received 11 April 2003, in final form 13 January 2004

Published 6 April 2004

Online at stacks.iop.org/MST/15/911 (DOI: 10.1088/0957-0233/15/5/019)

Abstract

This paper presents a novel non-contact vibration-monitoring technique based on transient measurements from a Fabry–Perot interferometric displacement sensor implemented using single-mode fibre. Two different extrinsic sensor configurations are demonstrated using one-fibre and two-fibre arrays of $4/125\ \mu\text{m}$ single-mode fibre butted with a gradient-index lens. The design concept, mathematical modelling and results are demonstrated. The sensor configurations exploit fringe discrimination over multiple orders. A working range up to $14\ \mu\text{m}$ is demonstrated for the measurement of vibration amplitude at 1 kHz excitation using the one-fibre configuration. Similar tests using the two-fibre configuration indicated a displacement measurement up to $65\ \mu\text{m}$ and vibration measurement up to $7\ \mu\text{m}$ at 2.5 kHz. The two-fibre configuration is also assessed in conjunction with an absolute scheme for the measurement of vibration using dual-wavelength signal processing. In this scheme, two wavelength signals are captured from the sensing interferometer to provide unambiguous measurement of vibration direction.

Keywords: vibration sensor, Fabry–Perot interferometer, microdisplacement sensor, single-mode fibre sensor

1. Introduction

Vibration monitoring of machinery is reducing the overall operating costs of industrial plants. If a monitoring system records the vibration history, changing levels of vibration over time would warn a plant engineer of the need for maintenance to prevent breakdown or serious damage. Piezoelectric transducers, however, have found limited application in harsh environments, such as electrical substations, due to their

propensity to malfunction in the presence of high voltages, high magnetic fields and aggressive atmospheres [1].

In contrast, fibre-optic sensors are excellent candidates for monitoring vibration in electromechanical equipment. The attractive feature of fibre-optic sensors is their ability to operate without interaction with electromagnetic fields, thus enabling them to be used by electricity utilities to monitor critical parameters. These sensors convey information as modulations of optical parameters such as intensity, phase and wavelength. Although intensity modulation is easy to implement, measurement error is likely due to spurious changes of signal strength. Optical phase is modulated by means of Michelson, Mach–Zehnder, Sagnac and Fabry–Perot

¹ T K Gangopadhyay was working in The University of Sydney, Australia from 1995 to 1999 and is presently doing research work in Central Glass & Ceramic Research Institute (CSIR), Calcutta-700 032, India.

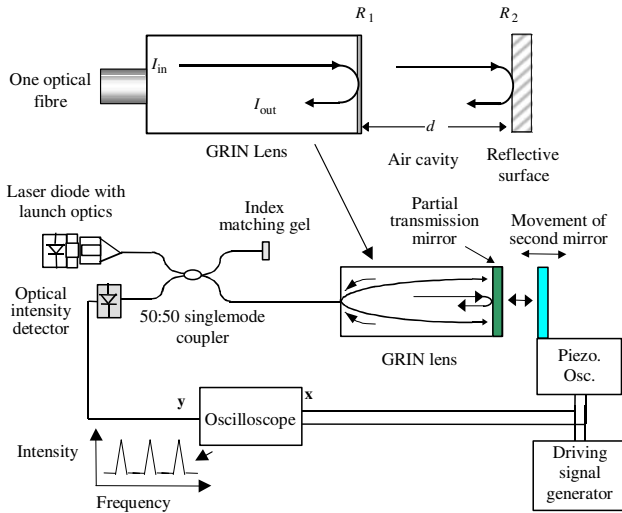


Figure 1. Geometry of a reflective FPI sensor butted with one fibre (top). Schematic of associated system including ray optics (bottom).

(FP) interferometers. In optical interferometry, coherent light is split between two paths so that a phase perturbation in one path causes a cyclical variation in the intensity of the recombined beam. Interferometric techniques are particularly attractive as they offer the highest measurement sensitivity, however, they suffer from lack of a direct linear phase read-out, random drifts in phase and polarization, and fluctuations in source intensity [2]. Nonetheless, several interferometers have been extensively used in fibre-optic sensing. Of these, the Fabry–Perot interferometer (FPI) has been shown to be highly sensitive to measurement errors caused by mechanical vibration, strain, temperature and acoustic waves [3–10].

In previous papers, we introduced a critical review on speckle-pattern-based vibration sensing in electromechanical equipment [11], a novel Fabry–Perot interferometric (FPI) sensor with multimode fibre transmission [12, 13] and with single-mode fibre transmission [14, 15] for measuring microdisplacement and vibration. This contribution presents new sensor configurations using two different arrays of single-mode fibre, compares the author’s design with the work of others, and demonstrates a dual-wavelength signal-processing scheme for the unambiguous measurement of vibration direction.

2. Vibration sensing based on Fabry–Perot interferometer

FPI is a versatile tool for fast and sensitive vibration analysis, which can be combined with fibre-optic signal transmission for rugged performance in harsh engineering environments. The FP cavity may simply be the space between two, typically parallel, mirror surfaces as shown in figure 1 (top). R_1 and R_2 are the reflectivities of the two mirrors. R_1 provides the reference signal, while R_2 moves with the target vibrations providing the sensing signal. This pair of mirrors creates a one-dimensional resonating optical cavity. The two reflected signals interfere constructively or destructively dependent on the cavity length d , and propagate back through the fibre to the detector. Movement of the second mirror changes d , thus

changing the interference. The reflected intensity I_R from the FPI can be expressed from the interference of superimposed signals from a two-wave interferometer [3, 4] as

$$I_R = A_1^2 + A_2^2 + 2A_1A_2 \cos \Delta\varphi \quad (1)$$

where A_1 and A_2 are the amplitude coefficients of the reflected signals due to R_1 and R_2 , and $\Delta\varphi$ is the phase difference between them. The round-trip phase-lag φ within such a cavity is given by [16, 17] as

$$\varphi = 4\pi nd \cos \theta / \lambda \quad (2)$$

where n is the refractive index of the medium between the mirrors, d is the mirror separation, θ is the angle of incidence and λ is the propagating wavelength. We assume an air-filled cavity and normal incidence ($n \approx 1$, λ is approximately its free-space value λ_0 and $\theta = 0$), so that $\varphi = 4\pi d / \lambda_0$. A phase change of 2π in the sensing signal corresponds to one fringe period, or a change in optical path difference (OPD) of λ_0 .

The contrast or sharpness of the fringes is determined by

$$F = 4R_1R_2 / (1 - R_1R_2)^2 \quad (3)$$

where F is the finesse of the cavity [18]. Low-finesse cavities, in which one or both mirror reflectivities (R_1 and R_2) are low, are commonly used in sensing applications. The operation of such cavities may be dominated by a single reflection.

2.1. Fringe-count method

As one fringe is equivalent to an OPD of λ_0 , it is also equivalent to a $\lambda_0/2$ mirror displacement in the reflective FPI configuration. The relative displacement D of the target surface is thus given by

$$D = N\lambda_0/2 \quad (4)$$

where N is the number of fringes. Due to the periodic output, fringe-counting methods [3] may be used to determine D over multiple wavelengths. Thus, at $\lambda_0 = 780$ nm, one fringe is equivalent to $D = 0.39 \mu\text{m}$.

3. Proposed extrinsic FPI sensing configurations

3.1. One-fibre approach

The proposed EFPI vibration-sensing configuration has been presented by the author [14] and is shown in figure 1. The sensor uses one single-mode $4/125 \mu\text{m}$ fibre pigtail butted to a gradient-index (GRIN) lens of 0.25 pitch and 1.8 mm diameter (Melles Griot, 06LGS114). The GRIN lens is used for efficient light-guiding between the fibre and the sensor. A coating of partial reflectivity R_1 on the output face of the GRIN lens provides the reference signal. A steel surface of reflectivity R_2 moves with the target vibrations, providing the sensing signal. The sensor pigtail is spliced to a 50:50 single-mode fibre-optic coupler. Light is provided by a pigtailed laser diode (SHARP LT024MD) emitting at 780 nm. Index matching gel inhibits back reflection from the unused coupler port.

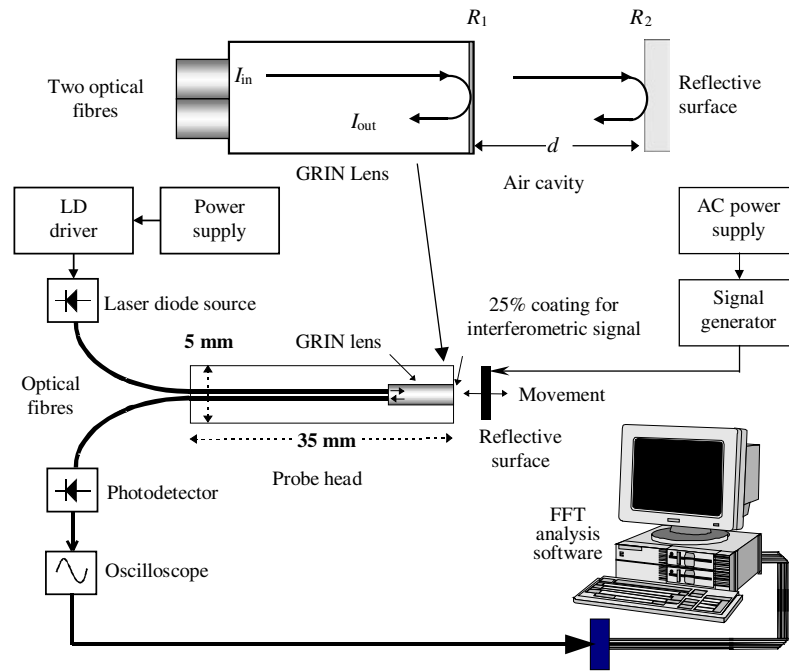


Figure 2. Geometry of a reflective FPI sensor butted with two fibres (top). Schematic of associated system including ray optics (bottom).

3.2. Two-fibre approach

The proposed two-fibre configuration is shown in figure 2. By utilizing two $4/125\ \mu\text{m}$ single-mode fibres, the system is significantly different from the multimode configuration presented earlier by the author [14]. In both cases, however, the second fibre is used to collect the signal reflected from the sensor, and thus no coupler is required.

4. Important features of the author's design

The author's design of vibration probe makes novel use of a coated GRIN lens butted to external transmitting optical fibres. The GRIN lens offers easy and efficient fibre to cavity coupling over a range of incident angles. The coating provides a reflectance of about 25%, which is substantially higher than the nominal value (4% Fresnel, <1% anti-reflection). This gives enhanced contrast of the interferometric fringes. A polished steel surface, which is attached to the target surface under investigation, provides great design flexibility.

4.1. Comparison of the author's design with the work of others

A literature review revealed no author describing precisely the system designs proposed here, although some features were employed by Murphy *et al* in 1991 [3]. In their system, the fibres defining the FP cavity were permanently fixed with epoxy. As claimed, it would be useful as a strain gauge, but not as a non-contact vibration measurement probe. Important differences of the author's proposed designs shown in figures 1 and 2 include:

- (i) The use of a coated GRIN lens to increase the intensity of the reference signal above that defined by a simple air–glass interface.

- (ii) The use of dissimilar reflection coefficients for the two mirror surfaces (i.e. $R_1 \neq R_2$) to maximize the fringe contrast, whilst maintaining low-finesse operation.
- (iii) The use of either one or two fibres butted to the GRIN lens for signal transmission.
- (iv) Likely applicability to non-contact operation. As discussed in section 7, non-contact measurement is a prime requirement when retrofitting sensors to electro-mechanical equipment such as electrical machines.

5. Sensor design and performance

In the one-fibre sensor configuration in figure 1 (top), a single fibre transmits the input signal and receives the output signal. It is placed on the axis with, and in the focal plane of, the GRIN lens. The collimated output is thus parallel to the GRIN lens axis, and the signals returned from the partial coating and the movable reflector always follow the same return path through the GRIN lens. Changes in optical path only occur within the cavity between the coating and the reflector as in a conventional FPI, thus resulting in the most efficient interference. With this arrangement, interferometric changes were obtained over displacements of hundreds of microns. An external fibre coupler is used to separate the input and output sensor signals.

In the two-fibre sensor configuration in figure 2 (top), the two fibre axes are equally disposed about that of the GRIN lens. In fact, they must be offset by at least one fibre radius—in this case $125\ \mu\text{m}$, taking into account the acrylate coating. The collimated cavity beam thus has a small angle of inclination. After a double passage through the GRIN lens, the reflected light is efficiently collected by the second fibre because it is at the mirror image location of the first.

The photodiode detectors are connected as shown in figures 1 and 2. After analogue detection, the signal is stored

on a digital oscilloscope (Nicolet Pro-42), and then processed by a computer.

5.1. GRIN lens

The purpose of the GRIN lens is fourfold. First, it provides a solid support on which to attach the transmission fibres. Second, it ensures efficient interference by collimating light within the FPI cavity. Third, it efficiently directs light reflected from the FPI into the end of the receiving fibre. Fourth, it provides a substrate on which to deposit a reflective coating to provide the interferometric reference. Unfortunately, the chosen GRIN lens was supplied with a <1% anti-reflection coating. This was too small to provide adequate fringe contrast. Removing this coating to recover the 4% Fresnel reflection still proved inadequate. A novel approach was finally implemented. This involved depositing a partially reflective coating on the output face of the GRIN lens. First, the anti-reflection coating was removed by Jung Precision Optics, Australia. Then a coating comprising a $\lambda/4$ film of Al_2O_3 , at 650 nm, was applied by Frances Lord Optics, Australia. This coating had a reflectance of 25% in order to match the intensities of the interfering signals, thereby giving fringes of maximum contrast. Finally, although GRIN lenses can exhibit bi-refractive problems, none were observed during this work.

5.2. Ray-path analysis of the GRIN lens

For a step-index single-mode fibre, an approximate empirical expression for the propagating spot size w is

$$w \approx a \left(0.65 + \frac{1.619}{V^{3/2}} + \frac{2.879}{V^6} \right) \quad (5)$$

where a is the core radius, and $0.8 \leq V \leq 2.5$ [19, 20]. The value of w is chosen in such a way that leads to the maximum launching efficiency of the exact fundamental mode field by an incident Gaussian field. In the present work, $V = 2.25$ at the $\lambda_0 = 780$ nm source wavelength (which is well within the well-known $V < 2.405$ criterion for single-mode operation). The fibre used also has $a = 2 \mu\text{m}$, and thus $w = 1.3 \mu\text{m}$ from equation (5). This light spot enters a GRIN lens whose refractive index profile n is given by

$$n(r) = n_0 \left[1 - \frac{1}{2} \delta^2 r^2 \right] \quad (6)$$

where r takes values up to the 0.9 mm lens radius, $n_0 = 1.603$ and $\delta = 0.339 \text{ mm}^{-1}$. Axial rays have a height x given by $x = x_0 \cos \delta z$ [19, 20]. And the spot size w_0 is given by [19, 20]

$$w_0 = \sqrt{\frac{\lambda_0}{\pi n_0 \delta}}. \quad (7)$$

Thus $w_0 = 21 \mu\text{m}$, which is much larger than the $1.3 \mu\text{m}$ spot size of the fibre. Figure 3 shows the envelope of ray paths propagating within the GRIN lens.

6. Experimental results and discussion

6.1. Results with the one-fibre configuration

For dynamic testing, the reflective steel surface was rigidly fixed to a piezoelectric transducer (PZT). The steel surface

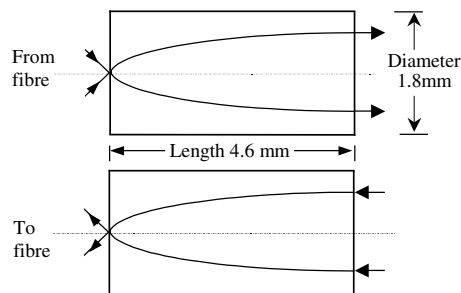


Figure 3. Ray envelope within the 0.25 pitch GRIN lens.

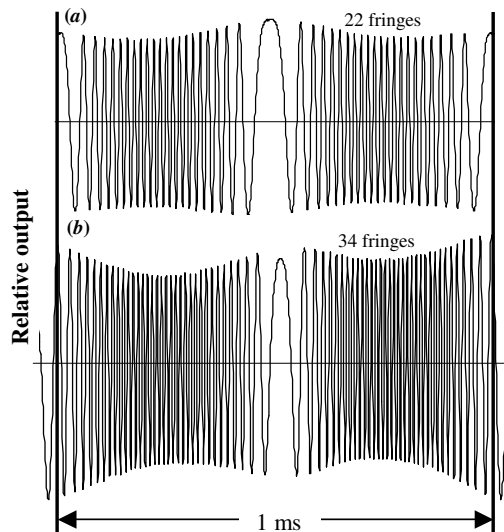


Figure 4. 1 kHz response of the EFPI sensor system with one single-mode fibre: (a) at $8.58 \mu\text{m}$ vibration amplitude ($\equiv 22$ fringes) and (b) at $13.26 \mu\text{m}$ vibration amplitude ($\equiv 34$ fringes).

and PZT combination were then aligned with respect to the sensor using a six-axis piezoelectric displacement stage. The PZT was driven by a sine-wave voltage from a programmable function generator. Interference fringes were recorded at various frequencies and amplitudes, resulting in distinct repeating patterns of fringes.

Figure 4 shows the fringe patterns obtained at low- and high-amplitude excitation at 1 kHz. At the low excitation there are 22 fringes and, from equation (4), the vibration displacement D is thus $8.58 \mu\text{m}$. At the high excitation, there are 34 fringes, which is equivalent to $D = 13.26 \mu\text{m}$. D is determined simply by counting the number of generated fringes.

Figure 5 shows that the number of generated fringes (and hence displacement) varies linearly with excitation of the PZT. The sensing arrangement is clearly suitable for dynamic monitoring over many fringe orders.

6.2. Results with the two-fibre configuration

By using separate launch and receive fibres, reflector movement distorts the ray paths through the GRIN lens. This results in a monotonically varying fringe contrast, which is of some use in determining direction over relatively large displacements of the reflector.

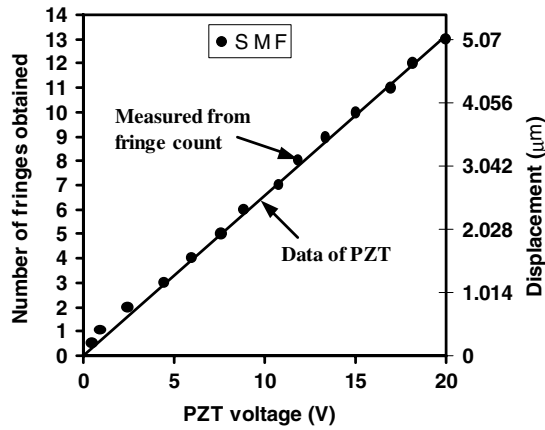


Figure 5. Number of fringes versus excitation for the EFPI sensor system with one single-mode fibre (SMF).



Figure 6. Displacement response of the EFPI sensor system with two single-mode fibres.

Displacement measurement. Using the alignment procedure described in section 6.1, the output of the interferometer was obtained as the reflector displaced $65 \mu\text{m}$ towards the GRIN lens. The resultant waveform (figure 6) exhibits a monotonically varying contrast of approximately 167 fringes.

Vibration measurement. The alignment and excitation procedures were used as described in section 6.1. Figure 7 shows the response to both low- and high-amplitude excitation at 2.5 kHz. The result is vibration displacements of $2.73 \mu\text{m}$ and $6.63 \mu\text{m}$ respectively.

Figure 8 shows that the number of generated fringes (and hence displacement) varies monotonically with excitation of the PZT. The sensing arrangement is thus suitable for dynamic monitoring over 10–20 fringe orders.

6.3. Response of the two-fibre sensor configuration to dual wavelength interrogation

This work used the same experimental set-up as shown in figure 2. The motivation to use dual-wavelength signal interrogation is to resolve the direction ambiguity observed in varying degrees in sections 6.1 and 6.2. By now using two wavelengths instead of one, a phase lead–lag phenomenon

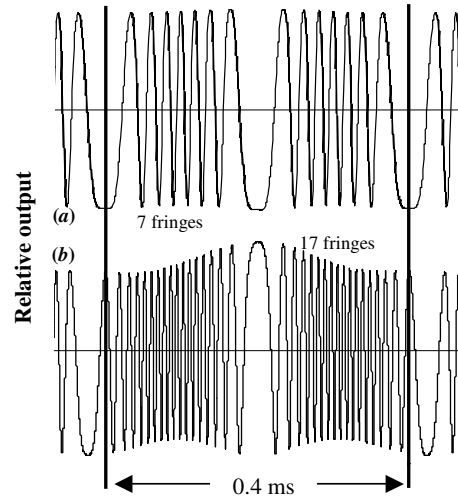


Figure 7. 2.5 kHz response of the EFPI sensor system with two single-mode fibres: (a) at $2.73 \mu\text{m}$ vibration amplitude ($\cong 7$ fringes) and (b) at $6.63 \mu\text{m}$ vibration amplitude ($\cong 17$ fringes).

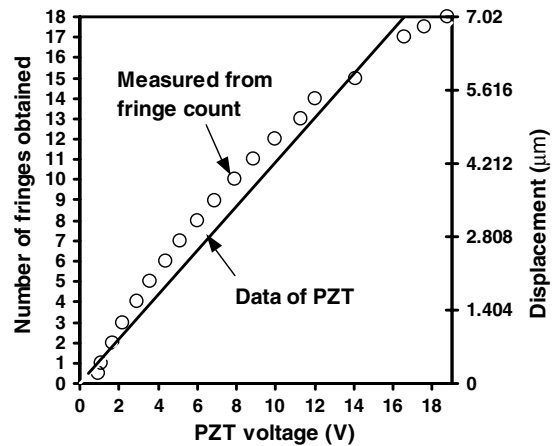


Figure 8. Number of fringes versus excitation for the EFPI sensor system with two single-mode fibres.

can be observed on the system output due to the change in wavelength. This lead–lag phenomenon can be tracked to determine the direction of motion of the vibrating body.

Dual-wavelength interrogation was achieved by current modulation of the laser diode. By varying the drive current from 50 mA and 70 mA, the output wavelength was seen to vary about its nominal 780 nm centre value. The author did not observe mode-hopping of the laser diode in this configuration. However, potential remedies would be to bias operation midway between adjacent hops, and to temperature-stabilize the laser diode.

For each driving current, the system output is stored. Figure 9 shows a set of results at a 1.6 kHz vibration of about $2.73 \mu\text{m}$ displacement. The phase lead–lag phenomenon is clearly seen about the point of inflection. These results demonstrate that the developed system faithfully responds to a change in wavelength of the source, and that phase lead–lag of the output is observable. Hence, an appropriate configuration of the developed system could be developed which would solve the direction ambiguity.

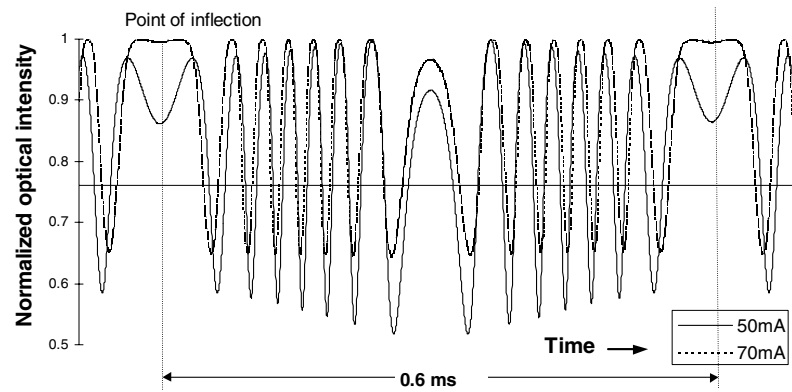


Figure 9. Oscilloscope showing the phase lead-lag phenomenon.

7. Conclusions

The operation of a simple, low-finesse, extrinsic FPI vibration sensor utilizing signal transmission via single-mode fibre has been presented. Movement between a highly-reflective and a partially-coated surface results in a change in intensity and phase of an interferometric signal from which displacement direction and vibration amplitude have been determined. The sensor exploits fringe discrimination over multiple orders. The demonstrated technique is a non-contact method for monitoring small vibrations of a moving surface.

The sensor utilizes single-mode fibre transmission and is more sensitive than a previous system using multimode fibres [12, 13]. The sensor has a cosinusoidal transfer function with high fringe contrast. The small dc component caused no processing difficulties.

A sensor configuration using one fibre was demonstrated to measure vibration up to $14\ \mu\text{m}$ at 1 kHz. Similarly, a configuration using two fibres was demonstrated to measure displacement up to $65\ \mu\text{m}$, and vibration up to $7\ \mu\text{m}$ at 2.5 kHz.

The two-fibre configuration was also assessed in conjunction with an absolute processing scheme for the measurement of vibration. This scheme employed dual-wavelength signal processing. The fringe waveforms associated with slightly different wavelengths are obtained by current modulation of a laser diode. The waveforms at the sensor output are thus captured demonstrating the potential for unambiguous measurement of vibration direction.

The presented sensor configurations are targeted towards applications needing measurement of small displacements with complete electrical isolation, such as in the electric power industry. However, the benefits of immunity to electromagnetic interference, electrical isolation, reflective probe configuration, small size and remote operation suggest many other application areas. Most of these areas need reflective extrinsic type of monitoring. Nonetheless, sensors suitable for use in high-vibration industrial environments need careful design. At a later stage, it would be desirable to make the entire system more compact and robust.

The sensor configurations reported in this paper are of simple design compared to other systems and are thus suitable for ruggedization suited to a much wider range of engineering environments.

Acknowledgments

TKG acknowledges the support of the Director, Central Glass and Ceramic Research Institute (CSIR), Calcutta, India, and the Australian Agency for International Development (presently AusAID). The author would like to acknowledge the advice of Associate Professor A D Stokes and the help of Dr G E Town of the School of Electrical and Information Engineering, Sydney, NSW 2006, Australia. The author would also like to thank Dr Philip J Henderson for his significant advice and suggestions on several occasions.

References

- [1] Lequime M 1997 Fibre sensors for industrial applications *12th Int. Conf. on Optical Fibre Sensors (OSA Technical Digest Series, vol 16) (OSA, Washington, DC)* pp 66–71
- [2] Sudarshanam V S 1992 New spectrum analysis technique for interferometric vibration measurement *Opt. Commun.* **88** 291–4
- [3] Murphy K A, Gunther M F, Vengsarkar A M and Claus R O 1991 Quadrature phase-shifted, extrinsic Fabry–Perot optical fibre sensors *Opt. Lett.* **16** 273–5
- [4] Murphy K A, Gunther M F, Wang A and Claus R O 1992 Extrinsic Fabry–Perot optical fibre sensor *Proc. 3th Optical Fibre Sensors Conf. (Monterey)* pp 193–6
- [5] Sudarshanam V S and Claus R O 1993 Split-cavity cross-coupled extrinsic fibre-optic interferometric sensor *Opt. Lett.* **18** 543–5
- [6] Coleman A J, Draguioti E, Tiptaf R, Shotri N and Saunders J E 1993 Acoustic performance and clinical use of a fibreoptic hydrophone *Ultrasound Med. Biol.* **24** 143–51
- [7] Ezbiri A and Tatam R P 1995 Passive signal processing for a miniature Fabry–Perot interferometric sensor with a multimode laser-diode source *Opt. Lett.* **20** 1818–20
- [8] Ezbiri A and Tatam R P 1996 Interrogation of low finesse optical fibre Fabry–Perot interferometers using a four wavelength technique *Meas. Sci. Technol.* **7** 117–20
- [9] Beard P C and Mills T N 1996 Extrinsic optical-fibre ultrasound sensor using a thin polymer film as a low-finesse Fabry–Perot interferometer *Appl. Opt.* **35** 663–75
- [10] Bhatia V, Murphy K A, Claus R O, Jones M E, Grace J L, Tran T A and Greene J A 1996 Optical fibre based absolute extrinsic Fabry–Perot interferometric sensing system *Meas. Sci. Technol.* **7** 58–61
- [11] Gangopadhyay T K and Henderson P J 1999 Prospects for speckle-pattern based vibration sensing in electromechanical equipment *Meas. Sci. Technol.* **10** R129–38

- [12] Gangopadhyay T K, Henderson P J and Stokes A D 1997 Vibration monitoring using a dynamic proximity sensor with interferometric encoding *J. Appl. Opt.* **36** 5557–61
- [13] Gangopadhyay T K and Henderson P J 1998 Interferometrically decoded fibre-optic vibration sensor using low-power laser diode *Technical Digest of Spring Topical Meeting of Optical Society of America—Laser Applications to Chemical and Environmental Analysis (Orlando, FL, 3–11 March)* vol 3 pp 34–6
- [14] Gangopadhyay T K and Henderson P J 1999 Vibration: history and measurement using an extrinsic Fabry–Perot sensor with solid-state laser interferometry *Appl. Opt.* **38** 2471–7
- [15] Gangopadhyay T K, Town G E and Stokes A D 1999 Noncontact vibration monitoring technique using a single-mode fibre sensor *Australian Conf. on Optical Fibre Technology (ACOFT-99) (Sydney, 4–9 July)*
- [16] Saleh B E A and Teich M C 1991 *Fundamentals of Photonics* (New York: Wiley)
- [17] Vaughan J M 1989 *The Fabry–Perot Interferometer: History, Theory, Practice and Applications* (Bristol: Adam Hilger)
- [18] Melles Griot 1990 *Optics Guide-5: The Practical Application of Light* (USA: Melles Griot) p 13.44
- [19] Marcuse D 1977 Loss analysis of single mode fibre splices *Bell Syst. Tech. J.* **56** 703
- [20] Ghatak A and Thyagarajan K 1999 *Introduction to Fibre Optics* (Cambridge: Cambridge University Press) p 150